Title
Synaptic Consolidation Normalizes AMPAR Quantal Size following MAGUK Loss

Journal
Neuron, 87(3)

ISSN
0896-6273

Authors
Levy, Jonathan M
Chen, Xiaobing
Reese, Thomas S
et al.

Publication Date
2015-08-01

DOI
10.1016/j.neuron.2015.07.015

Peer reviewed

HHS Public Access

Author manuscript

Neuron. Author manuscript; available in PMC 2016 August 05.

Published in final edited form as:

Neuron. 2015 August 5; 87(3): 534–548. doi:10.1016/j.neuron.2015.07.015.

Synaptic Consolidation Normalizes AMPAR Quantal Size following MAGUK Loss

Jonathan M. Levy[1,2], **Xiaobing Chen**[3], **Thomas S. Reese**[3], and **Roger A. Nicoll**[2,*]

[1]Neuroscience Graduate Program, University of California San Francisco, San Francisco, CA 94158, USA

[2]Department of Cellular and Molecular Pharmacology, University of California San Francisco, San Francisco, CA 94158, USA

[3]Laboratory of Neurobiology, National Institute of Neurological Disorders and Stroke, National Institutes of Health, Bethesda, MD 20892, USA

SUMMARY

The mechanisms controlling synapse growth and maintenance are of critical importance for learning and memory. The MAGUK family of synaptic scaffolding proteins is abundantly expressed at glutamatergic central synapses, but their importance in controlling the synaptic content of glutamate receptors is poorly understood. Here, we use a chained RNAi-mediated knockdown approach to simultaneously remove PSD-93, PSD-95, and SAP102, the MAGUKs previously shown to be responsible for synaptic localization of glutamate receptors. We find that MAGUKs are specifically responsible for creating functional synapses after initial spine formation by filling functionally silent spines with glutamate receptors. Removal of the MAGUKs causes a transient reduction in AMPA receptor quantal size followed by synaptic consolidation resulting in a normalization of quantal size at the few remaining functional synapses. Consolidation requires signaling through L-type calcium channels, CaM kinase kinase, and the GluA2 AMPA receptor subunit, akin to a homeostatic process.

INTRODUCTION

The glutamatergic synapse, consisting of a postsynaptic specialization with clustered glutamate receptors opposite a presynaptic terminal, is the site of fast excitatory neurotransmission in the brain. Proper formation of the postsynaptic specialization requires that glutamate receptors localize to the synapse and associate with the complex network of signaling and scaffolding molecules known as the postsynaptic density (PSD). The process

*Correspondence: roger.nicoll@ucsf.edu.

AUTHOR CONTRIBUTIONS

J.M.L. and X.C. designed experiments. T.S.R. and R.A.N. helped design experiments, interpret data, and supervised the project. J.M.L. performed all experiments and wrote the manuscript. X.C., T.S.R., and R.A.N. provided manuscript comments and directed revisions.

SUPPLEMENTAL INFORMATION

Supplemental Information includes Supplemental Experimental Procedures and four figures and can be found with this article online at http://dx.doi.org/10.1016/j.neuron.2015.07.015.

of glutamate receptor trafficking and localization has been extensively studied, and multiple lines of evidence demonstrate that the PSD scaffolding proteins themselves play an instructive role in regulating the localization of synaptic glutamate receptors (El-Husseini et al., 2000; Schnell et al., 2002). The primary protein family implicated in synaptic glutamate receptor localization is the four-member membrane-associated guanylyl kinase (MAGUK) family (Elias and Nicoll, 2007; Opazo et al., 2012): PSD-93, PSD-95, SAP97, and SAP102.

The MAGUKs are membrane-associated cytoplasmic scaffolding proteins that are highly enriched at the PSD and are ideally situated to serve as a bridge between glutamate receptors and cytoplasmic structural proteins, such as polymerized actin, that form the protein backbone of the dendritic spine. MAGUKs are anchored to the plasma membrane at postsynaptic specializations primarily by N-terminal palmitoylation, directly and indirectly bind glutamate receptors via PDZ binding domains, and link these receptors to the cytoplasmic protein scaffold with C-terminal SH3 and GK domains (Kim and Sheng, 2004). Germline knockout of single MAGUKs has little or no effect, but these results are confounded by compensation within the MAGUK family (Elias et al., 2006). RNAi-mediated knockdown, an acute manipulation, does not suffer from this drawback and offers greater insight into the endogenous role of MAGUKs. Acute overexpression or RNAi-mediated knockdown of PSD-93 or PSD-95 results in correlated changes in the number of synaptic AMPA-type glutamate receptors (AMPARs), demonstrating that MAGUKs play an instructive role in the localization of synaptic AMPARs (Chen et al., 2011; Ehrlich et al., 2007; Ehrlich and Malinow, 2004; Elias et al., 2006; Schlüter et al., 2006).

Reductions in PSD-93 or PSD-95 by RNAi-mediated knockdown cause loss of AMPAR-containing synapses. Strikingly, there is no deficit in the number of AMPARs at the remaining synapses, which has been interpreted to mean that individual synapses may each contain either PSD-93 or PSD-95 (Elias et al., 2006) or that the MAGUKs may be required primarily for the development of AMPAR-containing synapses (Ehrlich et al., 2007). Additionally, removal of several other scaffolding proteins present at all PSDs, including GKAP (Shin et al., 2012) and Shank1 (Hung et al., 2008), also results in all-or-none loss of AMPAR-containing synapses rather than uniform loss of some AMPARs from every synapse. While these data might suggest that synapses are highly heterogeneous and these scaffolding proteins each play a functional role at only a subset of synapses, a plausible alternative would be that loss of ubiquitous synaptic proteins from all synapses triggers a compensatory reorganization in a process resembling a homeostatic rearrangement in an effort to maintain the number of AMPARs at each synapse. The most obvious candidate pathway for this reorganization would be the canonical homeostatic pathway, in which signaling dependent on calcium entry through L-type voltage-gated calcium channels (LTCCs) (Ibata et al., 2008; Thiagarajan et al., 2005) acts on downstream targets including GluA2 (Gainey et al., 2009; Goold and Nicoll, 2010; but see Altimimi and Stellwagen, 2013).

The data from single-MAGUK manipulations have supported the hypothesis that MAGUKs function primarily as “slots” for AMPARs that control their synaptic abundance (Schnell et al., 2002; Shi et al., 2001). Knockdown of multiple MAGUKs, however, causes reductions in both AMPAR- and NMDAR-mediated transmission (Elias et al., 2006), suggesting

MAGUKs play a more fundamental role at the synapse: acting as basic scaffolding molecules localizing both classes of glutamate receptors. In this study, we have used a chained-miRNA approach to reduce expression of PSD-93, PSD-95, and SAP102 using RNAi-mediated knockdown. These results provide the first direct study of simultaneous knockdown of the MAGUKs shown to be responsible for synaptic localization of glutamate receptors. We find that knockdown of the three MAGUKs causes large decreases in both AMPAR and NMDAR transmission, with each of the three MAGUKs playing an equal role. This deficit results purely from a reduction in the number of synapses containing glutamate receptors without any decrease in synaptic strength of the remaining functional synapses or spine density. Furthermore, we show that the all-or-none loss of AMPARs is a result of "winner-take-all" synaptic consolidation, a process that acts to normalize quantal size. Remarkably, this process, which has not previously been described, implies that individual synapses have an intrinsic set point.

RESULTS

Pan-MAGUK Knockdown Reduces Synaptic AMPAR and NMDAR-Mediated Currents

To test whether the MAGUKs are necessary for glutamatergic transmission, we created a construct containing the CAG hybrid promoter driving expression of GFP and chained microRNAs targeting the three synaptic MAGUKs: PSD-93, PSD-95, and SAP102 (hereafter called the MAGUK miRNA, Figure 1A). The fourth member of the MAGUK family, SAP97, has been found not to play a role in baseline transmission (Howard et al., 2010) and was therefore initially excluded. Previous experiments exploring the role of the MAGUK family have been unable to make direct comparisons between neurons lacking MAGUKs and wild-type cells and have therefore suffered from an inability to quantify the effects of acute MAGUK removal directly. Viral infection of the MAGUK miRNA, using sequences that have previously been validated individually (Elias et al., 2006), substantially reduced protein levels of PSD-93, PSD-95, and SAP102 in dissociated hippocampal neurons (Figure 1B). To determine the functional consequences of MAGUK knockdown, we performed dual whole-cell recordings in rat hippocampal organotypic cultures. We biolistically transfected neurons with the MAGUK miRNA and identified transfected, GFP-expressing CA1 pyramidal neurons by morphology and location. We then stimulated Schaffer collaterals and performed simultaneous whole-cell recording of evoked excitatory postsynaptic currents (EPSCs) from pairs of transfected and neighboring untransfected control neurons. Expression of the MAGUK miRNA caused large and equivalent reductions in both AMPAR and NMDAR transmission (Figure 1C), leaving only a small glutamatergic EPSC. Importantly, viral infection of slice cultures via microinjection followed by dual whole-cell recording produced equivalent results (Figures S1A–S1C), validating our use of viral infection for our biochemical characterization (Figure 1B). A previous report using germline knockouts showed the MAGUKs have the ability to compensate for loss of several family members (Elias et al., 2006), and our knockdown strategy left open the possibility that SAP97, though it has no role in baseline function, might play a compensatory role. To determine whether SAP97 plays such a role, we transfected slice cultures from SAP97 knockout mice (Howard et al., 2010). There was no further reduction in transmission in SAP97 knockout mice compared to wild-type mice (Figures S1D–S1G), indicating that

SAP97 does not play a compensatory role. We therefore continued the study looking only at knockdown of PSD-93, PSD-95, and SAP102. Although our results demonstrate that MAGUKs are responsible for the large majority of synaptic glutamatergic current, it is difficult to ascertain the source of the remaining current. It could be due either to an incomplete removal of MAGUK protein or to a MAGUK-independent mechanism.

The reduction in both AMPAR and NMDAR transmission could be explained by changes in the three synaptic parameters: a presynaptic decrease in neurotransmitter release probability (P_r), a decrease in number of functional synapses (N), or a decrease in the postsynaptic response to glutamate, here likely due to a decrease in the number of glutamate receptors at each synapse (q). Several previous studies have found knockdown of PSD-95 causes solely a postsynaptic effect (Elias et al., 2006; Schlüter et al., 2006; but see Futai et al., 2007). To determine whether the removal of all three MAGUKs results in a presynaptic deficit, we measured the paired-pulse ratio, an indicator of neurotransmitter release probability, and found no change (Figure 1D). This result indicates that the decrease in fast glutamatergic transmission cannot be explained by changes in P_r and is due to either a decrease in the number of functional synapses, a decrease in the number of receptors per synapse postsynaptically, or a combination of the two effects.

All MAGUKs Play Roles in Baseline Glutamate Receptor Localization

Before further characterizing the general role of the MAGUK protein family, we first wanted to determine the contribution of each member to baseline fast excitatory transmission. Previous experiments (Elias et al., 2006) have reported that PSD-93 and PSD-95 each account for half of AMPAR-mediated transmission (but see Krüger et al., 2013), while SAP102 plays a compensatory role if both PSD-93 and PSD-95 are lost. Knockdown of PSD-93 or PSD-95 has been reported to have either no (Elias et al., 2006) or minimal effect (Ehrlich et al., 2007) on NMDAR currents. These single-knockdown results, combined with our data that the MAGUK miRNA has a significant effect on NMDAR currents, indicate that synaptic NMDARs are lost in significant numbers only when multiple MAGUKs are lost. To determine the individual contribution of each MAGUK family member in our system, we used miRNA constructs targeting each single MAGUK as described in Figure 1A, with a CAG promoter driving GFP followed by miRNA against PSD-93, PSD-95, or SAP102 in its 3′ UTR.

We find that knockdown of each MAGUK caused equivalent decreases in glutamatergic transmission. Removal of PSD-93, PSD-95, or SAP102 individually caused a decrease of about 50% in AMPAR and 25% in NMDAR transmission (Figures 2A–2C). Furthermore, the arithmetic addition of individual contributions of the MAGUKs to baseline AMPAR transmission (50% per MAGUK member, summing to an impossible 150%) results in an overestimate of the total contribution (Figure 2D). This suggests that removal of a small number of MAGUKs causes a disproportionately large reduction in AMPAR currents. Electron microscopy studies have shown that synapses with PSD diameter < 180 nm do not contain AMPARs and represent “silent synapses” (Takumi et al., 1999), suggesting that although small PSDs presumably contain MAGUKs, a primary component of the PSD (Chen et al., 2008; Sheng and Hoogenraad, 2007), PSDs with few MAGUKs cannot localize

AMPARs. Therefore, as MAGUKs are lost, AMPAR transmission will decrease disproportionately as many small MAGUK-containing synapses fall under the size threshold required to contain AMPARs (Takumi et al., 1999).

Incremental removal of MAGUKs results in a small reduction in NMDAR current that is additive, in contrast to the cooperative effects on AMPARs, with the triple MAGUK miRNA resulting in a decrease that is approximately three times as large as any single miRNA (Figure 2D). These results suggest that the relationship between MAGUK and NMDAR binding is roughly linear, with decreases in MAGUK abundance resulting in equivalent decreases in NMDAR content at synapses. This is in agreement with electron microscopy data showing NMDAR content is independent of PSD size (Takumi et al., 1999), meaning PSD size reductions do not cause reductions in NMDAR content. It is therefore likely that NMDAR EPSC reductions reflect loss of NMDAR-containing synapses. Additionally, we were surprised to find that knockdown of SAP102, which previously had been thought to be unnecessary for baseline transmission in organotypic rat slices (Elias et al., 2006), reduced both AMPAR and NMDAR currents, demonstrating a role for SAP102 in mediating baseline currents (Figure 2C).

Dependence of SAP102 Phenotype on Method of RNAi Delivery

What might account for the difference between our present results (Figure 2C), in which knockdown of SAP102 reduced both AMPAR and NMDAR currents, and previous published results, which found no effect (Elias et al., 2006)? One possible technical explanation for this disagreement could be the method of RNAi delivery in organotypic slices. We noticed a striking pattern in previous experiments: delivery of PSD-95 shRNA via viral transduction (Elias et al., 2006; Schlüter et al., 2006) did not decrease NMDAR current, while biolistic transfection of PSD-95 shRNA constructs (Ehrlich et al., 2007; Futai et al., 2007) caused a decrease in both AMPAR and NMDAR current. We reasoned that biolistic transfection might be more effective at knocking down endogenous protein, and we therefore explored whether the method of RNAi transfection might account for the difference.

If viral transduction with our SAP102 RNAi construct causes no deficit, it would suggest that the phenotype we see is specific to biolistic transfection and implicate the transfection method as the critical parameter. Although our biochemical results using virus in dissociated cultures (Figure 1B) show almost complete loss of MAGUK protein, we cannot directly extrapolate these data to slice culture, due to differences in the preparation and the transduction method, including potential differences in expression levels of the MAGUKs, differential expression of the CAG promoter, and differences in multiplicity of infection.

We therefore injected virus carrying our SAP102 knockdown construct into organotypic slice cultures and performed simultaneous whole-cell recordings. We found that, in contrast to the decrease seen following biolistic transfection, viral knockdown had no effect on AMPAR currents compared to controls, although there was a small but significant decrease in NMDAR current that differed significantly from the decrease seen following biolistic transfection (Figure 3A). We therefore conclude that the method of delivery controls the SAP102 phenotype. One possible explanation is the duration of knockdown; infection with

lentivirus may take effect more slowly than biolistic transfection. One alternate explanation, however, is the possibility that high miRNA expression levels could reveal off-target effects that were not strong enough to be functionally relevant at lower expression levels but now cause reductions in glutamatergic transmission. To determine whether biolistic transfection of SAP102 RNAi could be having off-target effects, we tested the SAP102 RNAi in slices from SAP102 germline knockout mice. Since the SAP102 protein has been genetically removed from all cells in this experiment, any differences between transfected and untransfected neurons caused by SAP102 miRNA transfection must be attributed to off-target effects on other proteins. As a control, we first confirmed our RNAi worked as expected in wild-type mice, causing a phenotype indistinguishable from that in rat (Figure 3B). In SAP102 knockout mice, we found biolistic transfection of SAP102 RNAi caused no change in either AMPAR or NMDAR transmission compared to controls (Figures 3C and 3D). We therefore conclude that our biolistic SAP102 knockdown phenotype in rat is due to a more efficient removal of SAP102 protein and not an off-target effect.

These results demonstrate that the method of RNAi transfection has important consequences for knockdown phenotypes and that biolistic transfection of RNAi results in more efficient removal of MAGUKs than viral transduction. Furthermore, they indicate that SAP102 contributes to baseline currents, which had not been previously observed and is now apparent due to a methodological improvement.

MAGUK Knockdown Causes Loss of Functional Glutamatergic Synapses

After finding that PSD-93, PSD-95, and SAP102 all play roles in baseline transmission, we returned to the initial finding that knockdown of all three proteins causes large reductions of both AMPAR and NMDAR-mediated currents (Figure 1C). These reductions could be due to a reduction in the number of functional synapses (N), a reduction in the number of glutamatergic receptors present at each synapse (q), or a mixture of the two. Determination of these quantal parameters requires analysis of glutamatergic transmission at individual synapses, usually done by miniature EPSC (mEPSC) analysis. We chose to measure evoked currents rather than mEPSCs and picked two complementary techniques to split evoked currents into their constituent quantal events. Each technique offered an advantage over mEPSC analysis: Sr^{2+}-evoked asynchronous EPSCs (aEPSCs) allowed us to link the quantal responses as closely as possible to the evoked currents we analyze elsewhere in this study, and coefficient of variation (CV) analysis allowed us to circumvent the electrical noise limit inherent in mEPSC recordings, which prevents observation of synapses containing few AMPARs.

To record aEPSCs, we replaced the Ca^{2+} normally present in the extracellular solution with equimolar Sr^{2+}. When Ca^{2+} is replaced with Sr^{2+}, synchronous transmitter release is replaced by asynchronous release, which lasts for a few hundred milliseconds after the stimulus (Miledi, 1966; Oliet et al., 1996; Xu-Friedman and Regehr, 2000). These aEPSCs are isolated quantal events. Analysis of the frequency (Figure 4A) and amplitude (Figure 4B) of aEPSCs from simultaneously recorded neurons yields information about quantal content ($N * P_r$) and quantal size (q), respectively. aEPSC frequency decreased following MAGUK knockdown (Figure 4C) with no difference in average a EPSC amplitude (Figure

4D), indicating that following MAGUK knockdown, quantal content has decreased with no change in quantal size. We additionally found no irregularities in the shape of the cumulative distribution functions for aEPSC amplitude and inter-event interval (Figures 4E and 4F), indicating changes are occurring at all synapses. A decrease in quantal content could be due to either a reduction in functional synapse number or probability of neurotransmitter release. Since MAGUK knockdown caused no change in the paired-pulse ratio (Figure 1D), the decrease in quantal content is due to a reduction in the number of functional synapses.

To complement our aEPSC data, we performed CV analysis on our EPSCs recorded in Ca^{2+}. This method of analysis utilizes the inherent variability in synaptic responses over many trials, which is caused by stochastic neurotransmitter release. By comparing the normalized variance in responses from two neurons receiving the same stimulus, it is possible to determine relative quantal size and quantal content. Changes in quantal size precisely change both the mean EPSC and the variance such that the normalized ratio of $mean^2$/variance, also known as $(coefficient\ of\ variation)^{-2}$ or CV^{-2}, remains constant. In contrast, changes in quantal content will cause proportional changes of equal magnitude in CV^{-2} (Bekkers and Stevens, 1990; Del Castillo and Katz, 1954; Gray et al., 2011; Malinow and Tsien, 1990; Marie et al., 2005). To demonstrate this principle in our preparation, we compared NMDAR EPSCs from control neurons before and after adding 1 μM D-APV, a sub-saturating concentration that blocks approximately half of all NMDARs, causing a reduction of about 50% in NMDAR EPSC (Figure S2A). The effect of this reduction on the variance can be visualized graphically by plotting mean EPSC against CV^{-2}. Average responses on the 45° line represent equivalent changes in EPSC and CV^{-2} and therefore pure changes in quantal content, while responses on the horizontal y = 1 line represent changes in EPSC amplitude without changes in variance and therefore represent changes in quantal size. In the case of D-APV, the ratio CV^{-2} is unchanged, as would be expected from uniform block of 50% of NMDARs at all synapses causing a reduction in quantal size (Figure S2B, re-plotted in Figure 4I). Analysis of evoked AMPAR (Figure 4G) and NMDAR (Figure 4H) currents following MAGUK knockdown in simultaneously recorded neurons showed equal reductions in CV^{-2} and mean EPSC (Figure 4I), suggesting that the decrease in mean EPSC was due to decreased quantal content, in agreement with our aEPSC data (Figures 4A–4F). We conclude that MAGUK knockdown results in a decrease in the number of functional synapses.

One finding that could explain a loss of functional synapses is a decrease in the number of dendritic spines, the cellular sites of excitatory synaptic contacts (Harris and Kater, 1994; Harris and Stevens, 1989). We therefore used confocal microscopy to compare spine density on the primary apical dendrites of control and MAGUK miRNA-expressing neurons. We found no difference in spine density between control and transfected neurons, suggesting that the MAGUKs play no role in spine formation (Figures S2C and S2D). This dissociation of the normally tight relationship between spines and functional synapses suggests that excitatory synaptic formation is mechanistically a two-step process consisting first of a spinogenic phase, in which the structural framework for a functional synapse is laid, and a subsequent synaptogenic phase, in which ionotropic receptors localize to the synapse using a MAGUK-dependent mechanism. To determine whether MAGUKs might play a role in

spine maintenance and maturation, we characterized spine morphology using super-resolution structured illumination microscopy (SIM). We find that MAGUK knockdown has no effect on spine neck length or diameter, but does significantly reduce spine head diameter (Figures S2E–S2H). Interestingly, this deficit in spine head diameter is mediated by a selective reduction in the number of spines with large heads, which presumably fail to mature in the absence of MAGUKs (Figures S2I and S2J). These results suggest that MAGUK loss curtails spine maturation. We therefore conclude that spine growth and maturation must have an initial MAGUK-independent phase followed by a MAGUK-dependent growth phase, likely an activity-dependent process dependent on the presence of a functional synapse. Finally, it has been suggested that the MAGUKs form complexes with extrasynaptic glutamate receptors (Rao et al., 1998). To determine whether MAGUKs might have a functional role in trafficking of glutamate receptors to the neuronal surface, we recorded whole-cell AMPAR and NMDAR currents (Figures S2K–S2N). We found no change, suggesting that the MAGUKs are not necessary for trafficking of glutamate receptors to the neuronal surface and instead are specifically necessary for synaptic localization of surface glutamate receptors.

L-Type Voltage-Gated Calcium Channels Are Required for Synaptic Consolidation

Loss of the MAGUKs causes reductions in AMPAR and NMDAR transmission (Figure 1C). The MAGUKs are a critical component of the PSD likely required for normal AMPAR transmission at all synapses. One simple prediction following loss of MAGUKs would therefore be uniform loss of AMPARs from every synapse resulting in a reduction of quantal size with little change in functional synapse number. Further analysis of the AMPAR transmission reduction, however, has found that it is due primarily to a reduction in the number of AMPAR-containing synapses with no change in quantal size (Ehrlich et al., 2007; this work, Figure 4; Elias et al., 2006). We therefore hypothesized that a compensatory mechanism must be acting to normalize quantal size, with the effect of converting the initial uniform removal of some AMPAR from every synapse into an all-or-none loss of synapses.

We reasoned that an active compensatory program would require a sensor of perturbed activity, and began by testing the involvement of the most well-characterized activity sensor: the L-type voltage-gated calcium channel (LTCC), a critical sensor of neuronal activity required for the activity of downstream homeostatic effector molecules. Homeostasis is induced by deviations in LTCC activity. Direct reduction in LTCC signaling via nifedipine application induces scaling up (Ibata et al., 2008; Thiagarajan et al., 2005; Wang et al., 2011), and increased excitation reduces synaptic currents via a mechanism requiring the LTCC (Goold and Nicoll, 2010). Together, these data indicate that the LTCC is required bi-directionally to maintain excitatory transmission. We reasoned that involvement of the LTCC in consolidation would suggest an active process at work akin to homeostasis working to maintain quantal size, while intact consolidation in the absence of LTCC signaling would imply the canonical homeostatic pathways were not involved. We biolistically transfected neurons with the MAGUK miRNA while blocking the activity of LTCCs in organotypic slice cultures by addition of nifedipine to the culture media. We found that knockdown of the MAGUKs in the presence of nifedipine caused large decreases

in AMPAR and NMDAR EPSCs compared to neighboring neurons (Figure 5A). This decrease did not differ significantly from the reductions caused by the MAGUK miRNA in the absence of nifedipine (Figures 5B and 5C, dashed line and shaded box indicate mean ± SEM of miRNA without nifedipine), indicating that LTCCs are not involved in mediating the effect of MAGUK knockdown. These results indicate that synaptic consolidation shifts AMPARs to normalize quantal size without a change in overall receptor number (model, Figure 7F). Finally, there was no change in the paired-pulse ratio, indicating that the addition of nifedipine did not change probability of release (Figure 5D).

CV^{-2} analysis demonstrates that in the presence of nifedipine, the reduction in AMPAR EPSCs caused by MAGUK miRNA is largely due to a reduction in quantal size (Figure 5E), in contrast to the reduction in quantal content caused by the MAGUK miRNA without nifedipine (Figure 4G). A small decrease in CV^{-2} remains, however, and indicates a small reduction in quantal content, possibly due to an across-the-board reduction in AMPAR content converting weak synapses to AMPAR-silent synapses. CV^{-2} analysis of NMDAR EPSCs shows a reduction in quantal content (Figure 5F) identical to that seen in the absence of nifedipine (Figure 4H), meaning that the all-or-none loss of NMDAR-containing synapses is not reliant on LTCC signaling. MAGUK miRNA data without nifedipine (Figure 4G) have been re-plotted to aid in comparison (Figure 5G). These results suggest that the AMPARs, but not NMDARs, undergo consolidation dependent on signaling by LTCCs following MAGUK knockdown.

Previous data showing the all-or-none loss following MAGUK removal have been collected following knockdown of a single member of the MAGUK family (Ehrlich et al., 2007; Elias et al., 2006). We have found knockdown of the entire MAGUK family leads to consolidation, but to directly determine whether consolidation acts following the milder disruption caused by removal of a single MAGUK family member, we knocked down PSD-95 in the presence of nifedipine. We find that knockdown of only PSD-95 causes consolidation, which is blocked by incubation in nifedipine, demonstrating that loss of a single MAGUK family member is sufficient to trigger consolidation (Figure 5H).

Since addition of nifedipine to the slice culture media affects both the transfected and neighboring neurons, we wanted to test whether consolidation could be rescued in a cell-autonomous manner. Our CV^{-2} analysis reports differences between transfected and control neurons and could be influenced by nifedipine acting on these controls. To confirm that LTCCs were acting to effect consolidation in the transfected neuron, we made use of cell-autonomous rescue with the nifedipine-insensitive T1036Y LTCC mutant (Dolmetsch et al., 2001; He et al., 1997), hereafter referred to as T1036Y. If LTCCs in the transfected neuron underlie consolidation, block of consolidation by nifedipine should be rescued by expression of T1036Y. We first confirmed surface expression of T1036Y by simultaneously measuring calcium currents in neurons biolistically transfected with T1036Y and neighboring untransfected neurons (Figure S3A), finding a large nifedipine-insensitive increase in current in neurons expressing T1036Y (Figures S3B–S3D). Expression of T1036Y with the MAGUK miRNA in the absence of nifedipine did not modulate the reduction in quantal content caused by MAGUK knockdown (Figure S3E). Co-expression of T1036Y and MAGUK miRNA in the presence of nifedipine rescued synaptic consolidation and resulted

in a reduction in AMPAR quantal content (Figures S3F and S3G). In all cases, there was no change in the magnitude of amplitude reduction in either AMPAR or NMDAR transmission compared to the MAGUK miRNA alone (Figures S3H–S3J), indicating that under these circumstances, nifedipine has no differential effect on synaptic transmission. These data also suggest that overexpression of CaV1.2 has no effect on synaptic transmission, in line with previous results (Wang et al., 2011), perhaps due to rate-limiting quantities of a downstream protein in the pathway.

Together, these results indicate that signaling pathways triggered by calcium flux through LTCCs are necessary for synaptic consolidation following knockdown of the MAGUKs. The involvement of LTCCs strongly suggests a two-step process by which MAGUK knockdown causes a reduction in quantal size, followed by a compensatory process resulting in a normalization of quantal size and reduction in quantal content. Furthermore, the manipulation of a signaling pathway via pharmacology without any additional structural perturbation indicates reorganization is an active, regulated process rather than a structural consequence of MAGUK protein loss.

Direct Electrophysiological Observation of Consolidation

Although incubation of miRNA-transfected slice cultures in nifedipine allowed us to infer that synaptic consolidation via L-type signaling must occur, we next attempted to strengthen this finding by directly observing neurons undergoing consolidation. We hypothesized that consolidation would occur on the same timescale as multiplicative synaptic scaling, a well-characterized form of homeostasis dependent on L-type signaling, which can induce homeostatic changes in less than 24 hr (Ibata et al., 2008; Turrigiano et al., 1998). As previous studies have shown the half-life of PSD-95 is approximately 36 hr (El-Husseini et al., 2002), recording within a few days of transfection, as would be required if consolidation happened on the same timescale as synaptic scaling, would not allow sufficient time for degradation of the existing protein. Instead, we took advantage of the finding that nifedipine blocks consolidation and incubated organotypic slices in nifedipine for 6 days, as done to test the involvement of LTCCs (Figures 5A–5H), which allows time for MAGUK protein degradation while blocking consolidation. Following 6 days in nifedipine, during which consolidation was blocked, slices were removed from nifedipine and recordings were done to assess the degree of consolidation on each subsequent day.

We found consolidation to be a linear process resulting in complete consolidation by 4 days following nifedipine washout (Figures 5I–5K; intermediate time points in Figures S3K and S3L). We additionally recorded from slices incubated in nifedipine with no washout to determine whether some consolidation might occur during this longer incubation despite the presence of nifedipine. We found no consolidation occurred in the presence of nifedipine (Figure S3M). These experiments establish a time course for consolidation. Although we are unable to measure consolidation that occurs directly after MAGUK knockdown, we infer that it relies on the same mechanism and occurs with the same kinetics. Additionally, these experiments demonstrate that consolidation can occur long after the loss of MAGUKs, further dissociating it from the initial EPSC reduction and showing that it is a separate compensatory process.

CaM Kinase Kinase Is Required for Consolidation of Synapses

We next attempted to identify targets of signaling through LTCC during consolidation. Previous work has determined that protein synthesis is necessary for certain forms of homeostatic plasticity and has specifically identified CaM Kinase 4 (CaMK4) as a transcriptional regulator that plays a role downstream of the LTCC (Goold and Nicoll, 2010; Ibata et al., 2008). Additionally, the relatively long period required for full consolidation suggests changes in protein synthesis may be required. The upstream CaMK4 regulator CaMKK (Soderling, 1999; Wayman et al., 2008) is an attractive target for testing whether CaMK4-mediated transcriptional regulation is necessary for consolidation, since both pharmacological inhibition and cell-autonomous rescue of inhibition via a drug-insensitive recombinant protein are possible. Inhibition of CaMKK by STO-609 (Tokumitsu et al., 2002) in slices transfected with the MAGUK miRNA hampered consolidation, resulting in a reduction in quantal size (Figures 6A and 6B). This deficit in consolidation was rescued by expression of CaMKK L233F, which is insensitive to STO-609 (Tokumitsu et al., 2003). Co-expression of MAGUK miRNA and CaMKK L233F in the presence of STO-609 resulted in consolidation indistinguishable from MAGUK miRNA alone, indicating that the deficit in consolidation is due to block of CaMKK signaling in the transfected neuron rather than a non-cell-autonomous result of incubation in STO-609 (Figures 6C and 6D). In agreement with previous work, CaMKK has no role in maintaining baseline transmission (Goold and Nicoll, 2010). Critically, incubation with STO-609, with or without co-expression of CaMKK L233F, had no effect on the reduction in AMPAR and NMDAR EPSCs caused by MAGUK knockdown (Figures 6E–6G).

These results indicate that signaling through the LTCC activates CaMKK. CaMK4, the major downstream target of CaMKK, plays a role in transcriptional regulation, most notably through the transcription factor CREB (Bito et al., 1997). We therefore conclude that, in agreement with the previously described role for CaMKK (Goold and Nicoll, 2010; Ibata et al., 2008), calcium influx through LTCCs leads to consolidation via changes in protein synthesis in a CaMKK/CaMK4-dependent manner. It is not possible, however, to directly test the necessity of translation in our system due to the relatively long time required for consolidation to occur.

GluA2 Is Required for Consolidation of Synapses following MAGUK Knockdown

The GluA2 AMPAR subunit has previously been implicated as an effector molecule in the homeostatic response to perturbations in cell activity levels (Gainey et al., 2009; Goold and Nicoll, 2010; but see Altimimi and Stellwagen, 2013), which in hippocampal neurons is expressed as a modulation of both quantal content and quantal size (Goold and Nicoll, 2010; Thiagarajan et al., 2002). It is therefore a promising candidate for involvement in quantal size re-normalization. To test whether the GluA2 subunit is involved, we knocked down the MAGUKs in organotypic slice cultures from GluA2 knockout animals (Jia et al., 1996) and assessed whether loss of GluA2 blocked the putative homeostatic consolidation of synapses. We would expect block of synapse consolidation to be expressed as a decrease in quantal size relative to control neurons. We found that CV analysis (Figures 7A–7C) and analysis of Sr^{2+}-evoked aEPSCs (Figures 7D and 7E) both revealed a decrease in quantal size. As seen with LTCC block, a small decrease in quantal content remains ($p < 0.05$). Much of the

observed reduction in aEPSC frequency (Figure 7D) is likely due to low-amplitude aEPSCs occurring below the noise threshold. In contrast, MAGUK knockdown in neurons from wild-type organotypic rat cultures causes no decrease in quantal size as measured by aEPSCs (Figures 4C and 4D) or CV analysis (Figures 4G–4I). Importantly, the relative decrease in EPSC amplitude is unchanged (Figure S4) compared to that seen in wild-type organotypic mouse cultures. We therefore conclude that synaptic consolidation uses machinery from the well-characterized homeostatic pathways, and the GluA2 AMPAR subunit is necessary for synaptic consolidation following MAGUK knockdown.

DISCUSSION

We find that the MAGUK family is of paramount importance in the localization of both AMPARs and NMDARs at excitatory glutamatergic synapses, as is demonstrated by the loss of most glutamatergic current following knockdown of PSD-93, PSD-95, and SAP102. We used a combination of approaches to characterize the role of MAGUKs in excitatory transmission. Analysis of spine density and surface glutamatergic currents indicate a specific role for MAGUKs in synaptic glutamate receptor localization separate from spine formation or receptor surface trafficking. Further characterization of the knockdown of all three MAGUKs reveals that the deficit in glutamatergic current is mediated by a postsynaptic reduction in the number of functional synapses. We go on to show that this reduction in synapse number is caused by a compensatory consolidation of synapses following MAGUK loss by a mechanism dependent on LTCCs, CaMKK, and GluA2, implicating a homeostasis-like pathway. Notably, the consolidation does not result in multiplicative synaptic scaling, demonstrating that the canonical homeostatic pathway likely plays additional roles. These findings extend previous work by demonstrating that MAGUKs, in addition to their previously reported role acting as “slots” for AMPARs, are a core component of the PSD with an equal role in regulating both types of glutamate receptors. Furthermore, we describe a compensatory pathway that utilizes the canonical homeostatic pathway and functions to oppose deviations in quantal size. This process implies that individual synapses have an intrinsic set point.

The Role of MAGUKs at the Postsynaptic Density

Our results suggest the MAGUKs play a specific functional role: localizing glutamate receptors to the PSD. We find no deficit in either surface spine density (Figures S2C and S2D) or receptor trafficking (Figures S2K–S2N), in agreement with previous results (Elias et al., 2008; but see Ehrlich et al., 2007). The MAGUK family has been suggested to act as a “slot protein” for AMPARs at the PSD, controlling the number of AMPARs present at synapses. This role, however, which has been characterized by single-MAGUK knockdown, does not preclude additional functions, and electron microscopy data showing that loss of PSD-95 causes disruption of the electron-dense PSD (Chen et al., 2008) suggest that beyond localizing synaptic glutamate receptors, MAGUKs are also responsible for localization of scaffolding and signaling proteins in the PSD. Furthermore, the initial biochemical characterization of MAGUK function found a direct interaction with NMDARs, not AMPARs (Kornau et al., 1995). Here, we find that knockdown of the three MAGUK family members together causes approximately an 80% reduction in both AMPAR and NMDAR

synaptic responses (Figure 1C). Although it is tempting to speculate that the remaining current is mediated by MAGUKs that have not been removed, it is worth noting that a previous study using a combination of knockout mice and RNAi-mediated knockdown to remove MAGUKs found a quantitatively similar reduction in AMPAR currents (Elias et al., 2006), opening the possibility that the remaining receptors may not require MAGUKs for localization.

The Role of MAGUKs in Synaptogenesis

One unresolved question in the study of synaptic development is the role and assembly order of proteins at the nascent synapse. Another group (Ehrlich et al., 2007) has found that knockdown of PSD-95 causes a loss of NMDAR current and a decrease in spine density, which they interpret as a role for MAGUKs in the initial formation of spines. In our hands, however, we find no decrease in spine density, suggesting that the MAGUKs do not play a role in the initial formation of spines, but are critical for filling the PSD with glutamate receptors. While the reasons for the differing results are unclear, several key differences in experimental approach exist. We believe that knockdown of the entire MAGUK family and observation of the resulting phenotype at a time point at which protein has been maximally removed provides the best chance for accurate assessment of the role of the MAGUK family. Our data demonstrate that synaptogenesis is mechanistically a two-step process, with an initial spinogenic step controlled by structural proteins such as neuroligin, whose loss causes a decrease in spine density (Chih et al., 2005; Shipman et al., 2011), and a second synaptogenic step dependent on MAGUKs that fills the spine with proteins that are necessary for a functional synapse. As we have not removed SAP97 during our anatomical experiments, however, we cannot rule out a role for SAP97 in spine formation but not synaptogenesis. One implication of this hypothesis is that spinogenic proteins cannot fully depend on MAGUKs for their localization. Proteins like Kalirin-7, which are thought to interact with PDZ-containing proteins and have been implicated in spine formation (Penzes et al., 2001), must have alternate mechanisms of localizing to the nascent spine. Furthermore, in agreement with previous results from mice lacking glutamate receptors (Lu et al., 2013), our data demonstrate that dendritic spines are maintained despite lacking functional glutamatergic synapses. Interestingly, we see a decrease in large-diameter spine heads with no decrease in quantal size. We speculate that these large-diameter spines may represent spines containing multiple PSDs, and their reduction reflects loss of an entire PSD, which would be reflected physiologically as a decrease in synapse number.

Synaptic Consolidation following MAGUK Loss

The decrease in quantal size following MAGUK knockdown in the GluA2 knockout and in slices treated with nifedipine or STO-609 suggests that the all-or-none synapse loss seen in untreated slices is the result of a two-step process: a loss of AMPARs from all functional synapses resulting in a quantal size decrease, followed by a compensatory consolidation of synapses, which increases quantal size back to baseline. Consolidation has the effect of preventing changes in quantal size and may be active throughout the life of the organism. Indeed, quantal size does not increase measurably over the life of the organism (Hsia et al., 1998), despite developmental increases in the amount of available synaptic scaffolding

proteins (Sans et al., 2000). Rather, quantal content increases with quantal size held constant, a phenomenon comparable to the consolidation observed in this study.

Consolidation requires LTCC activity, while nifedipine-induced scaling is induced by its absence. We believe this difference underlies the two separate effects of their shared pathway: consolidation maintains quantal size, while nifedipine-induced scaling increases it (Thiagarajan et al., 2005). Consolidation utilizes intact LTCC signaling, which maintains quantal size at baseline levels, to counteract the reduction in quantal size and bring synapses back to baseline quantal size. In contrast, nifedipine-induced scaling increases quantal size by disrupting the LTCC-dependent signal that maintains quantal size. Furthermore, MAGUK knockdown reduces the scaffolding proteins available before consolidation. This reduction means only a subset of synapses can be scaled up. Returning this subset to baseline quantal size comes at the cost of complete functional loss of other synapses, likely as scaffolding proteins consolidate at the “winning” synapses. While it is not clear what factors determine the winning synapses, only a subset of synapses maintain NMDARs (Figure 5G). Perhaps NMDAR-containing synapses would be favored in this competition.

How is consolidation maintained as an all-or-none effect? We propose that an active signal delivered via tonic LTCC activity to consolidated synapses maintains baseline quantal size and prevents loss of AMPARs to “losing,” functionally empty synapses to “scale up.” It cannot be that empty synapses lack the capacity to add glutamate receptors in this context, since neurons introduced to nifedipine after consolidation has occurred lose the tonic LTCC signal and no longer maintain consolidated synapses (Figures S3N and S3O). Therefore, active LTCC signaling maintains the “winner” of winner-take-all consolidation. In the absence of LTCC activity, no winner is generated or maintained and no imbalance in quantal size appears. Instead, AMPARs are distributed evenly and all synapses have relatively equal, reduced quantal sizes.

We have found that LTCCs, CaMKK, and the GluA2 subunit are required for consolidation, in line with previous evidence that they are required for homeostatic plasticity. The previously identified roles of the LTCC and CaMKK in transcription leave two possibilities for the role of GluA2. Either GluA2-containing receptors are an essential co-regulator, with LTCCs, of CaMKK-dependent transcription, or GluA2-containing receptors themselves are selectively modulated during the execution of homeostasis. In either case, proteins that selectively bind to GluA2, but not GluA1, such as GRIP, PICK1, and NSF (Bredt and Nicoll, 2003; Song and Huganir, 2002), are likely to underlie the selective reliance on GluA2, either by transducing a synaptic signal or by acting to change the abundance of GluA2 at the synapse.

Notably, the consolidation of synapses changes only the distribution of synaptic AMPARs, not their absolute number, as opposed to multiplicative synaptic scaling, which causes an overall increase in the absolute number of synaptic AMPARs in response to decreased activity. This process is therefore closely related but distinct from multiplicative synaptic scaling. The longer duration required for consolidation, 96 hr versus 24 hr for multiplicative scaling, further differentiates it. Indeed, although previous work (Sun and Turrigiano, 2011) has found activity-dependent synaptic scaling to be dependent on MAGUKs, they observe

an all-or-none loss of synapses following MAGUK knockdown, suggesting that, in agreement with our findings, the three synaptic MAGUKs are not necessary for synapse consolidation. The difference between synaptic consolidation and homeostasis suggests that in MAGUK-knockdown neurons, the machinery for determining “default” quantal size is intact even though the ability to change that set point via multiplicative scaling has been abolished. Following nifedipine washout, synapses in MAGUK miRNA-transfected neurons precisely return their quantal size to that of control neurons despite the overall decrease in excitatory input. This implies that synapses may function as autonomous homeostatic elements independent of neuronal-level homeostasis. While many lines of evidence show neuronal-level homeostasis in response to changes in firing rate, the mechanisms of synapse-level homeostasis are still being explored (reviewed in Lee et al., 2014). The canonical homeostatic pathway, best-studied in the context of neuron-level manipulations, is likely responsible for activating an array of related processes beyond neuron-level multiplicative scaling in response to activity perturbation. For example, the GluA2 subunit is necessary for proper distance-dependent scaling, a process which sets “default” quantal size, likely in a synapse-specific manner, and is an example of non-multiplicative scaling (Shipman et al., 2013).

These results clarify our understanding of the MAGUK family and reveal a compensatory pathway that activates in response to reductions in available MAGUK scaffolding protein. We demonstrate here the feasibility of knockdown of a protein family by simultaneously removing PSD-93, PSD-95, and SAP102. Given the ability of the MAGUKs to heterodimerize (Kim et al., 1996), we have created a reagent in the MAGUK miRNA that, when combined with overexpression of recombinant protein, provides the opportunity to perform detailed structure-function analyses of individual MAGUK family members on a background lacking endogenous MAGUKs. We additionally show a role for all three MAGUKs in mediating baseline transmission and show that a consolidation pathway locally normalizes synaptic strength while causing complete loss of a subset of functional synapses. Further exploration of this pathway will improve our understanding of the regulation of synaptic strength and may give insight into the remarkable finding that synaptic strength remains constant throughout development, even as synapse number and protein abundance change dramatically. Finally, these results imply that individual synapses autonomously maintain synaptic strength at an intrinsic set point.

EXPERIMENTAL PROCEDURES

Experimental Constructs

The triple MAGUK miRNA construct targeting PSD-93, PSD-95, and SAP102 was made using sequences that have been previously characterized (Elias et al., 2006). For calcium channel experiments, T1036Y mutation was made from human CaV1.2 cDNA (gift from D. Julius). See Supplemental Experimental Procedures for details.

Electrophysiology in Slice Cultures

Organotypic hippocampal slice cultures were made as described in Schnell et al., 2002. Slices from P6-P8 rats were biolistically transfected at 1–2 DIV (days in vitro). Where

specified, viral infections were performed via microinjection into the CA1 region using a Nanoject (Drummond Scientific) under manual control. Nifedipine (20 mM) or STO-609 (3 μM) was added at time of transfection. Recordings were performed at DIV 7–9 unless otherwise noted. Recordings and data analysis were performed as described in Supplemental Experimental Procedures.

Immunoblotting

Rat primary hippocampal dissociated neurons (E18.5) were infected with lentivirus expressing MAGUK miRNA construct or GFP alone at DIV 4–7. Neurons were harvested at DIV 17–18 in Tris-buffered saline (25 mM Tris [pH 7.4], 150 mM NaCl) plus 0.5% Triton-X and protease inhibitor mix (Roche Applied Sciences, cOmplete Protease Inhibitor Cocktail Tablets). Cell lysates were incubated at 4° for 30 min and centrifuged for 15 min at 12,000 *g*. Proteins were resolved by SDS-PAGE and analyzed by western blot with antibodies against PSD-93 (0.4 μg/ml, Neuromab clone N18/30), PSD-95 (1 μg/ml, Neuromab K28/43), SAP102 (2 μg/ml, Neuromab N19/2), and actin (0.2 μg/ml, Millipore C4).

Lentivirus Production

Three T-75 flasks of rapidly dividing HEK293T cells (ATCC) were transfected with 27 μg FUGW-MAGUK miRNA or FUGW, plus helper plasmids pVSV-G (18 μg) and psPAX2 (27 μg) using FuGENE HD (Promega). DNA was incubated with 210 μl FuGENE HD in 4.5 ml Opti-MEM (Life Technologies) before transfection, according to the manufacturer's directions. Forty hours later, supernatant was collected, filtered, and concentrated using the PEG-it Virus Precipitation Solution (System Biosciences) according to the manufacturer's directions. The resulting pellet was resuspended in 400 μl Opti-MEM or PBS, flash-frozen, and stored at −80° C.

Supplementary Material

Refer to Web version on PubMed Central for supplementary material.

ACKNOWLEDGMENTS

We thank W. Swat for the SAP97 mice, D. Julius for the human CaV 1.2 cDNA, and T. Soderling for the CaMKK cDNA. We thank K. Bjorgan and M. Cerpas for technical assistance, and all members of the Nicoll laboratory for discussion of and comments on the manuscript. This work was supported by grants from the U.S. National Institute of Mental Health.

REFERENCES

Altimimi HF, Stellwagen D. Persistent synaptic scaling independent of AMPA receptor subunit composition. J. Neurosci. 2013; 33:11763–11767. [PubMed: 23864664]

Bekkers JM, Stevens CF. Presynaptic mechanism for long-term potentiation in the hippocampus. Nature. 1990; 346:724–729. [PubMed: 2167454]

Bito H, Deisseroth K, Tsien RW. Ca2+-dependent regulation in neuronal gene expression. Curr. Opin. Neurobiol. 1997; 7:419–429. [PubMed: 9232807]

Bredt DS, Nicoll RA. AMPA receptor trafficking at excitatory synapses. Neuron. 2003; 40:361–379. [PubMed: 14556714]

Chen X, Winters C, Azzam R, Li X, Galbraith JA, Leapman RD, Reese TS. Organization of the core structure of the postsynaptic density. Proc. Natl. Acad. Sci. USA. 2008; 105:4453–4458. [PubMed: 18326622]

Chen X, Nelson CD, Li X, Winters CA, Azzam R, Sousa AA, Leapman RD, Gainer H, Sheng M, Reese TS. PSD-95 is required to sustain the molecular organization of the postsynaptic density. J. Neurosci. 2011; 31:6329–6338. [PubMed: 21525273]

Chih B, Engelman H, Scheiffele P. Control of excitatory and inhibitory synapse formation by neuroligins. Science. 2005; 307:1324–1328. [PubMed: 15681343]

Del Castillo J, Katz B. Quantal components of the end-plate potential. J. Physiol. 1954; 124:560–573. [PubMed: 13175199]

Dolmetsch RE, Pajvani U, Fife K, Spotts JM, Greenberg ME. Signaling to the nucleus by an L-type calcium channel-calmodulin complex through the MAP kinase pathway. Science. 2001; 294:333–339. [PubMed: 11598293]

Ehrlich I, Malinow R. Postsynaptic density 95 controls AMPA receptor incorporation during long-term potentiation and experience-driven synaptic plasticity. J. Neurosci. 2004; 24:916–927. [PubMed: 14749436]

Ehrlich I, Klein M, Rumpel S, Malinow R. PSD-95 is required for activity-driven synapse stabilization. Proc. Natl. Acad. Sci. USA. 2007; 104:4176–4181. [PubMed: 17360496]

El-Husseini AE, Schnell E, Chetkovich DM, Nicoll RA, Bredt DS. PSD-95 involvement in maturation of excitatory synapses. Science. 2000; 290:1364–1368. [PubMed: 11082065]

El-Husseini, Ael.-D.; Schnell, E.; Dakoji, S.; Sweeney, N.; Zhou, Q.; Prange, O.; Gauthier-Campbell, C.; Aguilera-Moreno, A.; Nicoll, RA.; Bredt, DS. Synaptic strength regulated by palmitate cycling on PSD-95. Cell. 2002; 108:849–863. [PubMed: 11955437]

Elias GM, Nicoll RA. Synaptic trafficking of glutamate receptors by MAGUK scaffolding proteins. Trends Cell Biol. 2007; 17:343–352. [PubMed: 17644382]

Elias GM, Funke L, Stein V, Grant SG, Bredt DS, Nicoll RA. Synapse-specific and developmentally regulated targeting of AMPA receptors by a family of MAGUK scaffolding proteins. Neuron. 2006; 52:307–320. [PubMed: 17046693]

Elias GM, Elias LAB, Apostolides PF, Kriegstein AR, Nicoll RA. Differential trafficking of AMPA and NMDA receptors by SAP102 and PSD-95 underlies synapse development. Proc. Natl. Acad. Sci. USA. 2008; 105:20953–20958. [PubMed: 19104036]

Futai K, Kim MJ, Hashikawa T, Scheiffele P, Sheng M, Hayashi Y. Retrograde modulation of presynaptic release probability through signaling mediated by PSD-95-neuroligin. Nat. Neurosci. 2007; 10:186–195. [PubMed: 17237775]

Gainey MA, Hurvitz-Wolff JR, Lambo ME, Turrigiano GG. Synaptic scaling requires the GluR2 subunit of the AMPA receptor. J. Neurosci. 2009; 29:6479–6489. [PubMed: 19458219]

Goold CP, Nicoll RA. Single-cell optogenetic excitation drives homeostatic synaptic depression. Neuron. 2010; 68:512–528. [PubMed: 21040851]

Gray JA, Shi Y, Usui H, During MJ, Sakimura K, Nicoll RA. Distinct modes of AMPA receptor suppression at developing synapses by GluN2A and GluN2B: single-cell NMDA receptor subunit deletion in vivo. Neuron. 2011; 71:1085–1101. [PubMed: 21943605]

Harris KM, Kater SB. Dendritic spines: cellular specializations imparting both stability and flexibility to synaptic function. Annu. Rev. Neurosci. 1994; 17:341–371. [PubMed: 8210179]

Harris KM, Stevens JK. Dendritic spines of CA 1 pyramidal cells in the rat hippocampus: serial electron microscopy with reference to their biophysical characteristics. J. Neurosci. 1989; 9:2982–2997. [PubMed: 2769375]

He M, Bodi I, Mikala G, Schwartz A. Motif III S5 of L-type calcium channels is involved in the dihydropyridine binding site. A combined radioligand binding and electrophysiological study. J. Biol. Chem. 1997; 272:2629–2633. [PubMed: 9006896]

Howard MA, Elias GM, Elias LA, Swat W, Nicoll RA. The role of SAP97 in synaptic glutamate receptor dynamics. Proc. Natl. Acad. Sci. USA. 2010; 107:3805–3810. [PubMed: 20133708]

Hsia AY, Malenka RC, Nicoll RA. Development of excitatory circuitry in the hippocampus. J. Neurophysiol. 1998; 79:2013–2024. [PubMed: 9535965]

Hung AY, Futai K, Sala C, Valtschanoff JG, Ryu J, Woodworth MA, Kidd FL, Sung CC, Miyakawa T, Bear MF, et al. Smaller dendritic spines, weaker synaptic transmission, but enhanced spatial learning in mice lacking Shank1. J. Neurosci. 2008; 28:1697–1708. [PubMed: 18272690]

Ibata K, Sun Q, Turrigiano GG. Rapid synaptic scaling induced by changes in postsynaptic firing. Neuron. 2008; 57:819–826. [PubMed: 18367083]

Jia Z, Agopyan N, Miu P, Xiong Z, Henderson J, Gerlai R, Taverna FA, Velumian A, MacDonald J, Carlen P, et al. Enhanced LTP in mice deficient in the AMPA receptor GluR2. Neuron. 1996; 17:945–956. [PubMed: 8938126]

Kim E, Sheng M. PDZ domain proteins of synapses. Nat. Rev. Neurosci. 2004; 5:771–781. [PubMed: 15378037]

Kim E, Cho KO, Rothschild A, Sheng M. Heteromultimerization and NMDA receptor-clustering activity of Chapsyn-110, a member of the PSD-95 family of proteins. Neuron. 1996; 17:103–113. [PubMed: 8755482]

Kornau HC, Schenker LT, Kennedy MB, Seeburg PH. Domain interaction between NMDA receptor subunits and the postsynaptic density protein PSD-95. Science. 1995; 269:1737–1740. [PubMed: 7569905]

Krüger JM, Favaro PD, Liu M, Kitlinska A, Huang X, Raabe M, Akad DS, Liu Y, Urlaub H, Dong Y, et al. Differential roles of postsynaptic density-93 isoforms in regulating synaptic transmission. J. Neurosci. 2013; 33:15504–15517. [PubMed: 24068818]

Lee KF, Soares C, Béïque JC. Tuning into diversity of homeostatic synaptic plasticity. Neuropharmacology. 2014; 78:31–37. [PubMed: 23541721]

Lu W, Bushong EA, Shih TP, Ellisman MH, Nicoll RA. The cell-autonomous role of excitatory synaptic transmission in the regulation of neuronal structure and function. Neuron. 2013; 78:433–439. [PubMed: 23664612]

Malinow R, Tsien RW. Presynaptic enhancement shown by whole-cell recordings of long-term potentiation in hippocampal slices. Nature. 1990; 346:177–180. [PubMed: 2164158]

Marie H, Morishita W, Yu X, Calakos N, Malenka RC. Generation of silent synapses by acute in vivo expression of CaMKIV and CREB. Neuron. 2005; 45:741–752. [PubMed: 15748849]

Miledi R. Strontium as a substitute for calcium in the process of transmitter release at the neuromuscular junction. Nature. 1966; 212:1233–1234. [PubMed: 21090447]

Oliet SH, Malenka RC, Nicoll RA. Bidirectional control of quantal size by synaptic activity in the hippocampus. Science. 1996; 271:1294–1297. [PubMed: 8638114]

Opazo P, Sainlos M, Choquet D. Regulation of AMPA receptor surface diffusion by PSD-95 slots. Curr. Opin. Neurobiol. 2012; 22:453–460. [PubMed: 22051694]

Penzes P, Johnson RC, Sattler R, Zhang X, Huganir RL, Kambampati V, Mains RE, Eipper BA. The neuronal Rho-GEF Kalirin-7 interacts with PDZ domain-containing proteins and regulates dendritic morphogenesis. Neuron. 2001; 29:229–242. [PubMed: 11182094]

Rao A, Kim E, Sheng M, Craig AM. Heterogeneity in the molecular composition of excitatory postsynaptic sites during development of hippocampal neurons in culture. J. Neurosci. 1998; 18:1217–1229. [PubMed: 9454832]

Sans N, Petralia RS, Wang YX, Blahos J 2nd, Hell JW, Wenthold RJ. A developmental change in NMDA receptor-associated proteins at hippocampal synapses. J. Neurosci. 2000; 20:1260–1271. [PubMed: 10648730]

Schlüter OM, Xu W, Malenka RC. Alternative N-terminal domains of PSD-95 and SAP97 govern activity-dependent regulation of synaptic AMPA receptor function. Neuron. 2006; 51:99–111. [PubMed: 16815335]

Schnell E, Sizemore M, Karimzadegan S, Chen L, Bredt DS, Nicoll RA. Direct interactions between PSD-95 and stargazin control synaptic AMPA receptor number. Proc. Natl. Acad. Sci. USA. 2002; 99:13902–13907. [PubMed: 12359873]

Sheng M, Hoogenraad CC. The postsynaptic architecture of excitatory synapses: a more quantitative view. Annu. Rev. Biochem. 2007; 76:823–847. [PubMed: 17243894]

Shi S, Hayashi Y, Esteban JA, Malinow R. Subunit-specific rules governing AMPA receptor trafficking to synapses in hippocampal pyramidal neurons. Cell. 2001; 105:331–343. [PubMed: 11348590]

Shin SM, Zhang N, Hansen J, Gerges NZ, Pak DT, Sheng M, Lee SH. GKAP orchestrates activity-dependent postsynaptic protein remodeling and homeostatic scaling. Nat. Neurosci. 2012; 15:1655–1666. [PubMed: 23143515]

Shipman SL, Schnell E, Hirai T, Chen BS, Roche KW, Nicoll RA. Functional dependence of neuroligin on a new non-PDZ intracellular domain. Nat. Neurosci. 2011; 14:718–726. [PubMed: 21532576]

Shipman SL, Herring BE, Suh YH, Roche KW, Nicoll RA. Distance-dependent scaling of AMPARs is cell-autonomous and GluA2 dependent. J. Neurosci. 2013; 33:13312–13319. [PubMed: 23946389]

Soderling TR. The Ca-calmodulin-dependent protein kinase cascade. Trends Biochem. Sci. 1999; 24:232–236. [PubMed: 10366852]

Song I, Huganir RL. Regulation of AMPA receptors during synaptic plasticity. Trends Neurosci. 2002; 25:578–588. [PubMed: 12392933]

Sun Q, Turrigiano GG. PSD-95 and PSD-93 play critical but distinct roles in synaptic scaling up and down. J. Neurosci. 2011; 31:6800–6808. [PubMed: 21543610]

Takumi Y, Ramírez-León V, Laake P, Rinvik E, Ottersen OP. Different modes of expression of AMPA and NMDA receptors in hippocampal synapses. Nat. Neurosci. 1999; 2:618–624. [PubMed: 10409387]

Thiagarajan TC, Piedras-Renteria ES, Tsien RW. alpha- and betaCaMKII. Inverse regulation by neuronal activity and opposing effects on synaptic strength. Neuron. 2002; 36:1103–1114. [PubMed: 12495625]

Thiagarajan TC, Lindskog M, Tsien RW. Adaptation to synaptic inactivity in hippocampal neurons. Neuron. 2005; 47:725–737. [PubMed: 16129401]

Tokumitsu H, Inuzuka H, Ishikawa Y, Ikeda M, Saji I, Kobayashi R. STO-609, a specific inhibitor of the Ca(2+)/calmodulin-dependent protein kinase kinase. J. Biol. Chem. 2002; 277:15813–15818. [PubMed: 11867640]

Tokumitsu H, Inuzuka H, Ishikawa Y, Kobayashi R. A single amino acid difference between alpha and beta Ca2+/calmodulin-dependent protein kinase kinase dictates sensitivity to the specific inhibitor, STO-609. J. Biol. Chem. 2003; 278:10908–10913. [PubMed: 12540834]

Turrigiano GG, Leslie KR, Desai NS, Rutherford LC, Nelson SB. Activity-dependent scaling of quantal amplitude in neocortical neurons. Nature. 1998; 391:892–896. [PubMed: 9495341]

Wang HL, Zhang Z, Hintze M, Chen L. Decrease in calcium concentration triggers neuronal retinoic acid synthesis during homeostatic synaptic plasticity. J. Neurosci. 2011; 31:17764–17771. [PubMed: 22159093]

Wayman GA, Lee YS, Tokumitsu H, Silva AJ, Soderling TR. Calmodulin-kinases: modulators of neuronal development and plasticity. Neuron. 2008; 59:914–931. [PubMed: 18817731]

Xu-Friedman MA, Regehr WG. Probing fundamental aspects of synaptic transmission with strontium. J. Neurosci. 2000; 20:4414–4422. [PubMed: 10844010]

Highlights

- MAGUK loss causes an all-or-none reduction in functional synapses
- MAGUK loss triggers consolidation, a process that maintains synaptic strength
- Consolidation maintains individual synapses at an intrinsic set point
- Consolidation depends on the L-type calcium channel, CaMKK, and GluA2

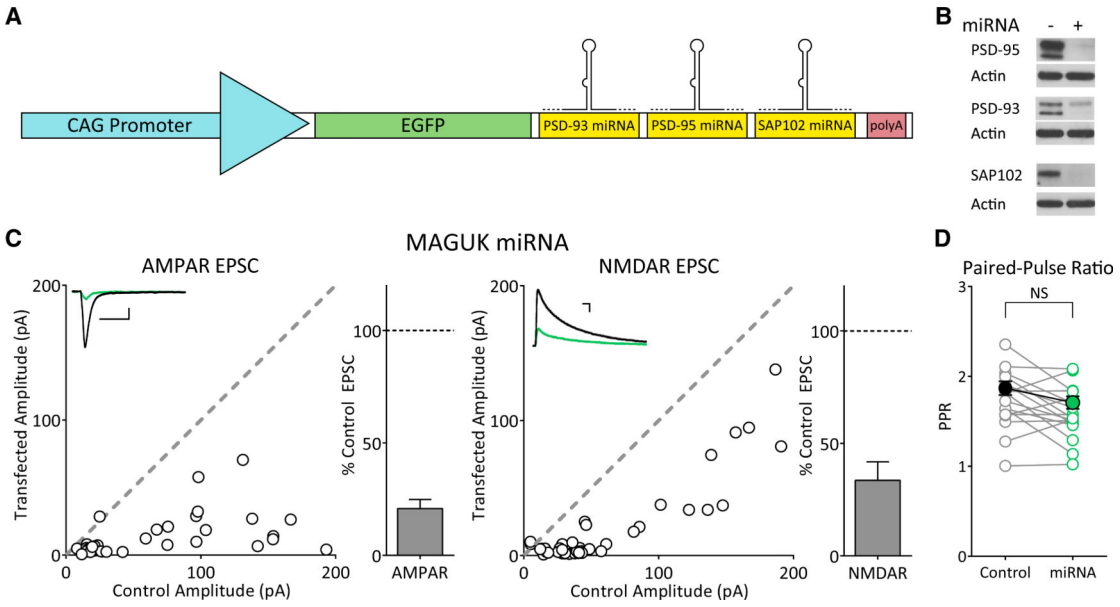

Figure 1. Pan-MAGUK Knockdown Reduces Synaptic AMPAR and NMDAR-Mediated Currents

(A) CAG hybrid promoter drives EGFP with a synthetic 3′ UTR containing miRNA hairpins against PSD-93, PSD-95, and SAP102.

(B) Infection of dissociated hippocampal neurons with lentivirus expressing the MAGUK miRNA construct results in reductions in the amount of PSD-95, PSD-93, and SAP102 protein without any change in the loading control actin.

(C) Scatter plots showing reductions in AMPAR and NMDAR EPSCs in MAGUK miRNA-transfected neurons compared to untransfected controls (AMPAR, 20.84% ± 4.03% control, $p < 0.005$, $n = 41$; NMDAR, 33.59% ± 8.22% control, $p < 0.005$, $n = 41$). Scatter plots of EPSCs show single pairs (open circles). Bar graphs show mean ratio ± SEM. AMPAR scale bars represent 25 ms, 25 pA; NMDAR scale bars represent 100 ms, 25 pA.

(D) No change in paired-pulse ratio (PPR), defined as second EPSC over first EPSC (Ctrl 1.75 ± 0.07, Expt 1.59 ± 0.06; $p > 0.05$, $n = 17$). Scale bars represent 25 pA, 50 ms. See also Figure S1.

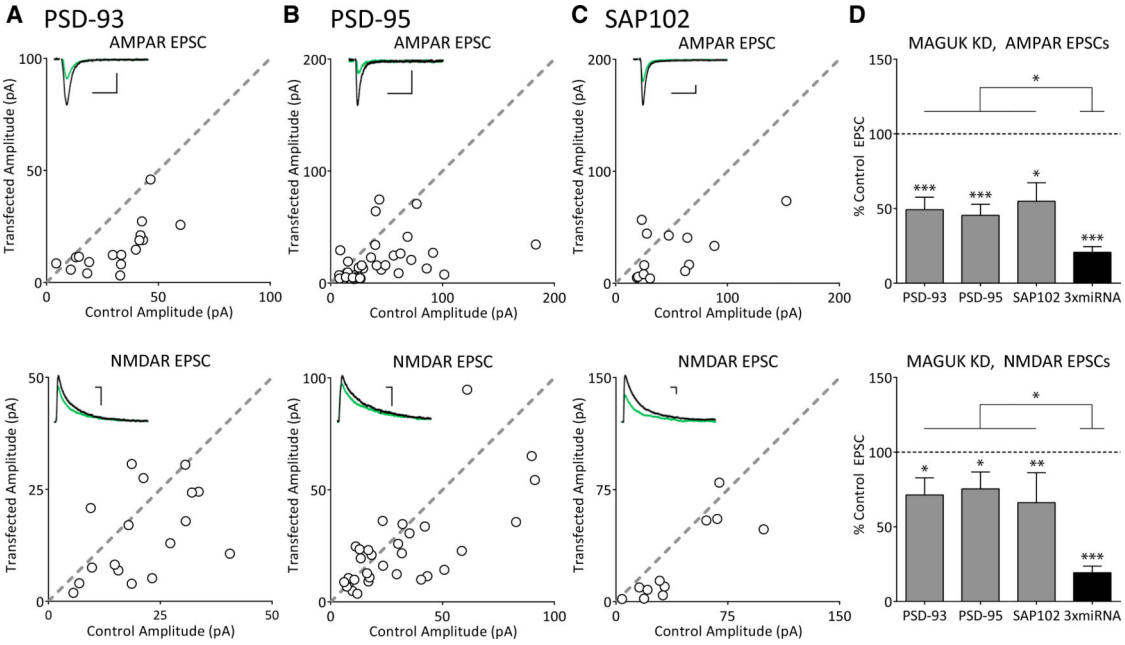

Figure 2. All MAGUKs Play Roles in Baseline Glutamate Receptor Localization

(A) PSD-93 knockdown causes decrease of AMPAR-mediated current (49.23% ± 8.34% control, $p < 0.005$, $n = 17$) and NMDAR-mediated current (71.34% ± 11.44% control, $p < 0.05$, $n = 17$).

(B) PSD-95 knockdown causes decrease of AMPAR-mediated current (45.38% ± 7.457% control, $p < 0.005$, $n = 34$) and NMDAR-mediated current (75.38% ± 11.37% control, $p < 0.05$, $n = 31$).

(C) SAP102 knockdown causes decrease of AMPAR-mediated current (54.83% ± 12.45% control, $p < 0.05$, $n = 13$) and NMDAR-mediated current (63.74% ± 20.07% control, $p < 0.01$, $n = 11$).

(D) Summary graphs of mean ± SEM. EPSC amplitudes, expressed as a percentage of control EPSC values.

Open circles represent amplitudes for single pairs. Scale bars represent 25 pA, 50 ms.

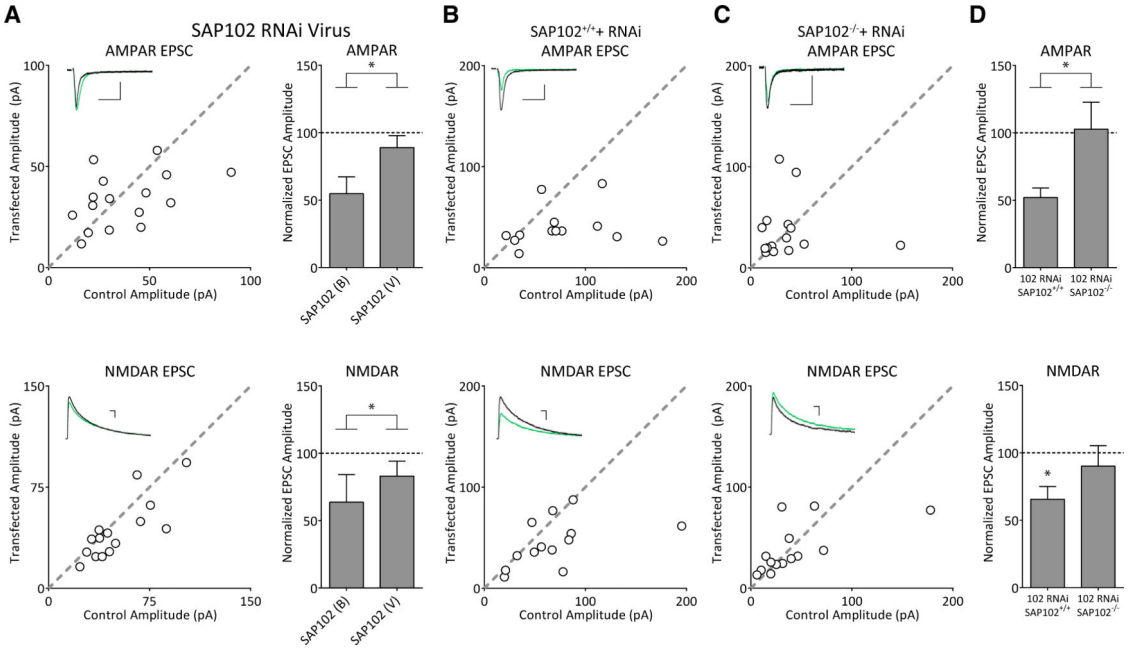

Figure 3. Dependence of SAP102 Phenotype on Method of RNAi Delivery

(A) SAP102 knockdown by viral transduction does not decrease AMPAR currents (88.95% ± 8.87% control, $p > 0.05$, n = 16), in contrast to biolistic knockdown (54.83% ± 12.45% control) (biolistics versus virus $p < 0.05$, n = 13 biolistics; n = 16 virus). SAP102 knockdown by viral transduction slightly decreases NMDAR currents (83.03% ± 11.04% control, $p < 0.05$, n = 15). Biolistic knockdown (63.74% ± 20.07% control) results in a greater decrease of NMDAR currents (biolistics versus virus $p < 0.01$, n = 11 biolistics; n = 15 virus).

(B) Biolistic knockdown of SAP102 in wild-type mice causes a decrease of AMPAR-mediated current (52.03% ± 7.06% control, $p < 0.01$, n = 13). Biolistic knockdown of SAP102 in wild-type mice causes a decrease of NMDAR-mediated current (65.58% ± 9.49% control, $p < 0.05$, n = 13).

(C) Biolistic knockdown of SAP102 in SAP102 knockout mice results in no change in AMPAR-mediated currents (102.70% ± 20.06% control, $p > 0.05$, n = 15) or NMDAR-mediated currents (90.16% ± 15.22% control, $p > 0.05$, n = 14).

(D) Knockdown of SAP102 in wild-type mice causes a statistically significant decrease in AMPAR-mediated current compared to knockdown in SAP102 knockout mice (wild-type versus KO $p < 0.05$, n = 13 WT, n = 15 KO). Knockdown of SAP102 in wild-type mice causes a statistically significant decrease in NMDAR current compared to controls, but not compared to knockdown in SAP102 knockout mice, although there is a trend toward significance (wild-type versus KO $p > 0.05$, n = 13 WT, n = 14 KO).

Open circles represent amplitudes for single pairs. Scale bars represent 25 pA, 50 ms.

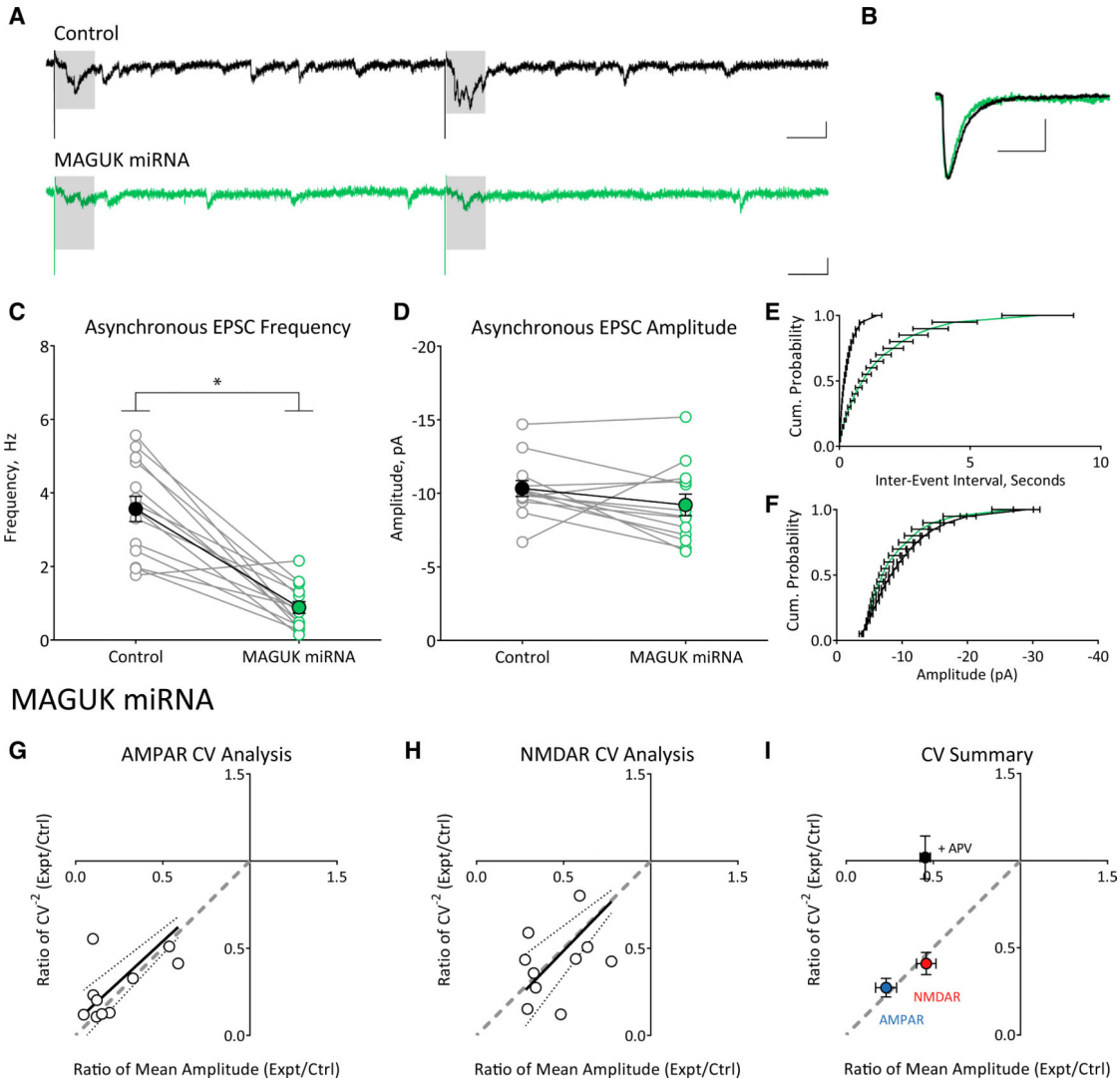

Figure 4. MAGUK Knockdown Causes Loss of Functional Glutamatergic Synapses

(A) Representative sample traces of asynchronous EPSCs (aEPSCs) recorded in the presence of Sr^{2+} in neurons expressing MAGUK miRNA or control neurons. 50 ms following stimulation (gray box) was excluded from analysis. Scale bars represent 50 ms, 15 pA.

(B) Representative average aEPSC traces showing no change in average amplitude. Black trace is control; green trace is experimental. Scale bars represent 20 ms, 4 pA.

(C) aEPSC frequency in neurons expressing MAGUK miRNA. Plot shows single pairs (open circles) and mean ± SEM (filled circles). aEPSC frequency is significantly reduced ($p < 0.05$) in neurons expressing MAGUK miRNA.

(D) aEPSC amplitude in neurons expressing MAGUK miRNA. Plot as in (C). There is no change in amplitude between control and MAGUK miRNA neurons ($p = 0.15$, $n = 13$).

(E and F) Cumulative distribution plots of aEPSC frequency and amplitude. Control shown in black, experimental in green. Cumulative distribution functions show no irregularities.

(G and H) Coefficient of variation analysis of simultaneously recorded pairs of control/miRNA neurons. CV^{-2} graphed against ratio of mean amplitude within each pair. Results along the horizontal y = 1 line are consistent with change in quantal size (q), results along gray dashed identity (45°) line are consistent with change in quantal content ($N \times P_r$). Analysis of AMPAR and NMDAR responses suggests decrease is due to reduction in quantal content. Small solid and dashed lines indicate linear regression line and 95% confidence intervals, respectively.

(I) Summary of coefficient of variation analysis. Both AMPAR and NMDAR average fall on the identity line ($p < 0.05$ versus horizontal line), while average response after D-APV falls on horizontal y = 1 line ($p > 0.05$). See also Figure S2.

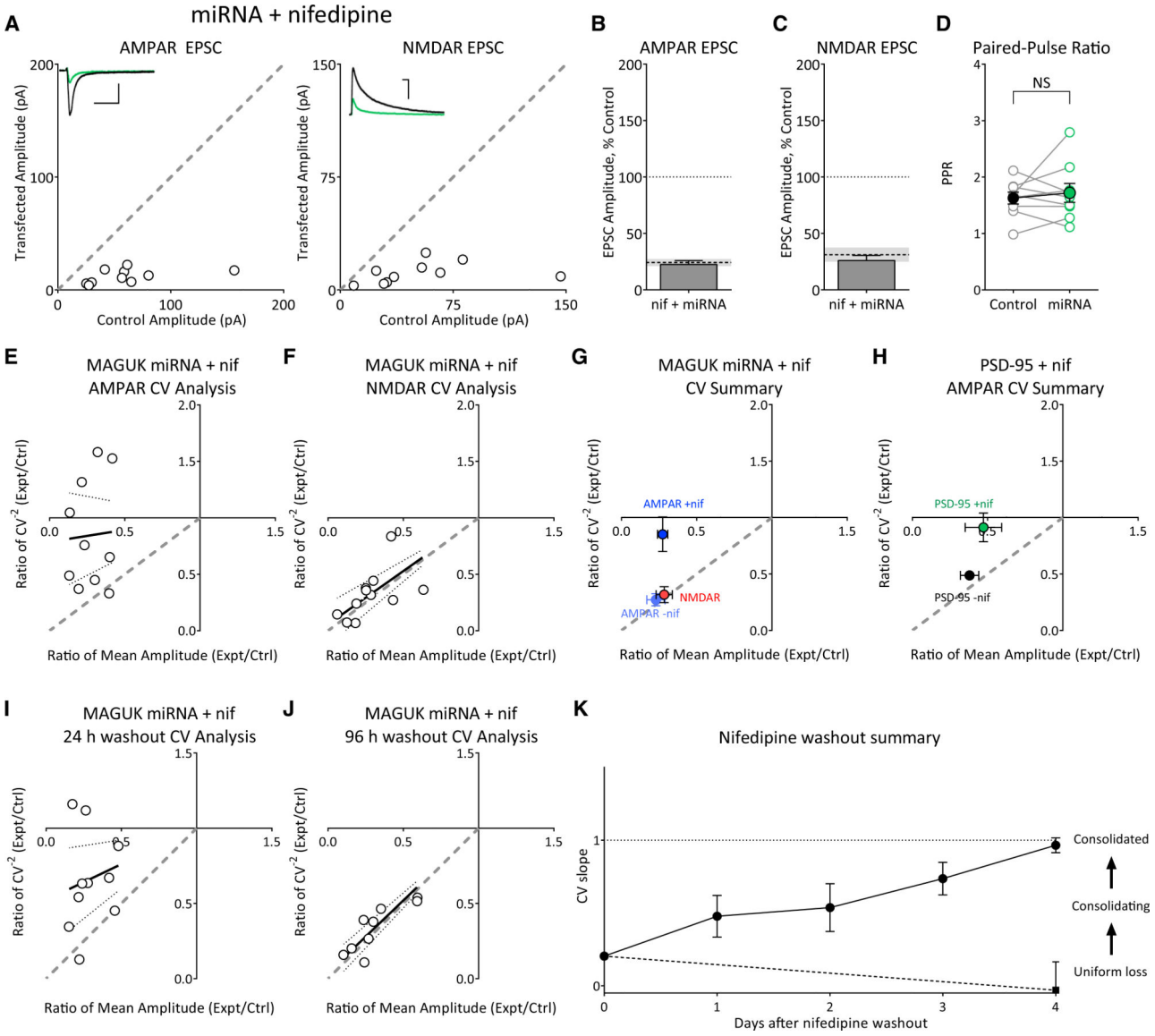

Figure 5. L-Type Calcium Channels Are Required for Synaptic Consolidation

(A) MAGUK miRNA transfection in the presence of 20 μM nifedipine causes significant reductions in both AMPAR and NMDAR EPSCs compared to neighboring untransfected neurons (AMPAR 20.17% ± 3.24%; NMDAR 21.35% ± 4.17%; n = 10 and $p < 0.05$ for both).

(B and C) Summary data showing no additional change in AMPAR or NMDAR EPSCs in MAGUK miNRA-expressing neurons with nifedipine compared to MAGUK miRNA alone ($p > 0.05$ for both). Dashed line and shaded area show mean ± SEM of normalized synaptic responses for MAGUK miRNA without nifedipine.

(D) No change in paired-pulse ratio (PPR), defined as second EPSC over first EPSC (Ctrl 1.63 ± 0.11, Expt 1.72 ± 0.17; $p > 0.05$, n = 9).

(E and F) Coefficient of variation analysis of simultaneously recorded pairs of control/miRNA neurons. CV^{-2} graphed against ratio of mean amplitude within each pair. Results along the horizontal line are consistent with change in quantal size (q), results along identity

(45°) line are consistent with change in quantal content ($N \times P_r$). Decrease in AMPAR EPSC is due to reduction in quantal size. Decrease in NMDAR EPSC is due to reduction in quantal content. Small solid and dashed lines indicate linear regression line and 95% confidence intervals, respectively.

(G) Summary of coefficient of variation analysis. AMPAR average falls near the horizontal line ($p < 0.05$ compared to horizontal line) and NMDAR average falls on the identity line. Data from MAGUK miRNA without nifedipine incubation (Figure 4G) are re-plotted to aid comparison.

(H) Coefficient of variation analysis of simultaneously recorded pairs of control/PSD-95 miRNA neurons (black circle) shows the reduction in AMPAR EPSC is due to reductions in quantal content. Reduction in AMPAR EPSC following PSD-95 knockdown and nifedipine incubation (green circle) is due to reductions in quantal size.

(I and J) Coefficient of variation analysis of simultaneously recorded pairs of control/miRNA neurons either 24 hr (I) or 96 hr (J) after nifedipine washout. Twenty-four hours after washout, the decrease in AMPAR EPSC is due to reductions in quantal content and quantal size. Ninety-six hours after nifedipine washout, the decrease in AMPAR EPSC is due to pure reduction in quantal content.

(K) Summary graph showing slope of CV dataset regression line versus hours post-nifedipine washout. As a control, nifedipine was not washed out of some slices (dashed line and black square). See also Figure S3.

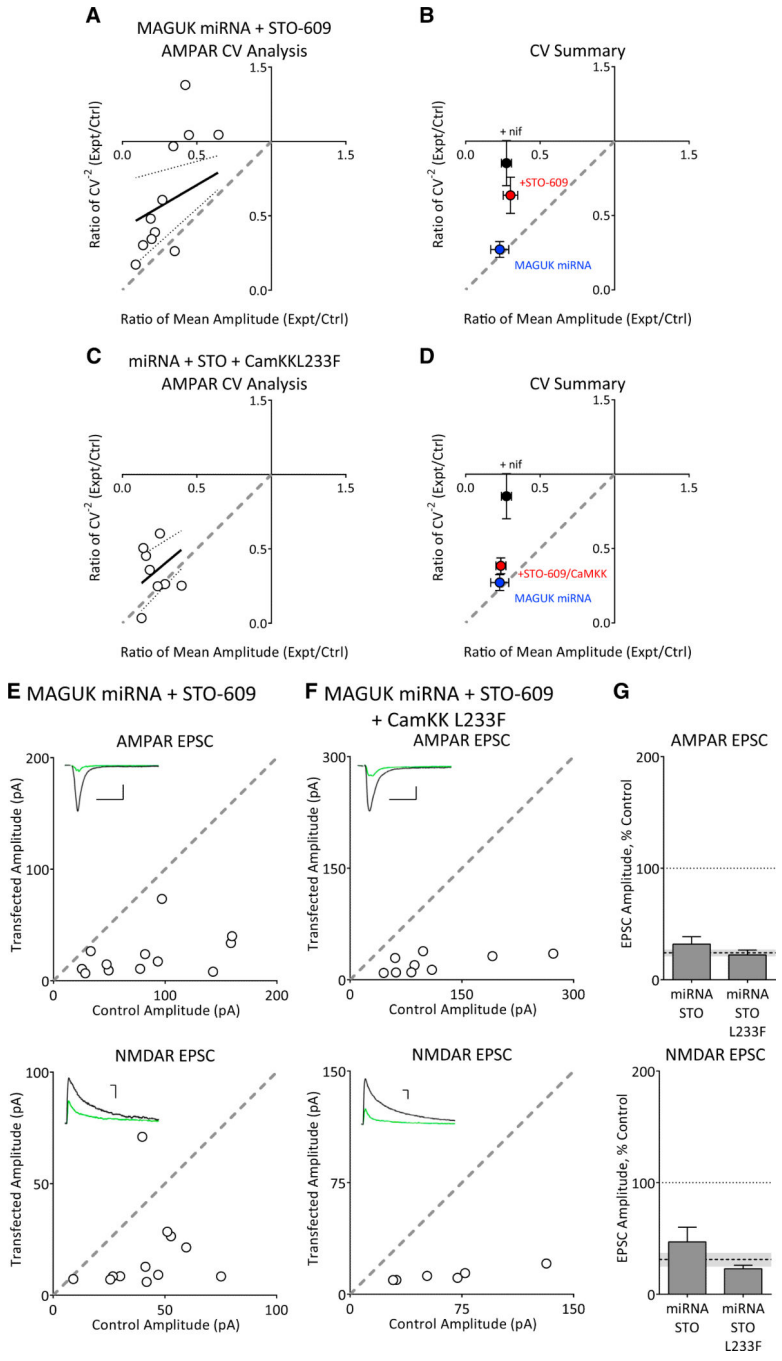

Figure 6. CaM Kinase Kinase Is Required for Synaptic Consolidation

(A) Coefficient of variation analysis of simultaneously recorded pairs of control/miRNA neurons in slices incubated with 3 μM STO-609. The decrease in AMPAR EPSCs is due to reduction in quantal size and quantal content. Small solid and dashed lines indicate linear regression line and 95% confidence intervals, respectively.

(B) Summary of coefficient of variation analysis. Data from MAGUK miRNA alone (Figure 4G), and plus nifedipine incubation (Figure 5E), are re-plotted to aid comparison.

(C) Coefficient of variation analysis of simultaneously recorded pairs of control/miRNA + CaMKK L233F neurons in slices incubated in STO-609. The decrease in AMPAR EPSC is due to reduction in quantal content.

(D) Summary of coefficient of variation analysis. Data from MAGUK miRNA alone (Figure 4G), and plus nifedipine incubation (Figure 5E), are re-plotted to aid comparison.

(E) MAGUK miRNA transfected in the presence of 3 μM STO-609 causes reductions in both AMPAR and NMDAR EPSC (AMPAR 31.93% ± 6.66%, n = 12; NMDAR 46.98.1% ± 13.14%, n = 12; $p < 0.05$ for both).

(F) MAGUK miRNA co-transfected with STO-609 insensitive CaMKK L233F in the presence of STO-609 causes reductions in both AMPAR and NMDAR EPSC (AMPAR 22.31% ± 4.32%, n = 9; NMDAR 22.86% ± 3.14%, n = 6; $p < 0.05$ for both).

(G) Summary data showing no additional change in AMPAR EPSC reduction due to incubation in STO-609 and co-expression of CaMKK L233F ($p > 0.05$ for all).

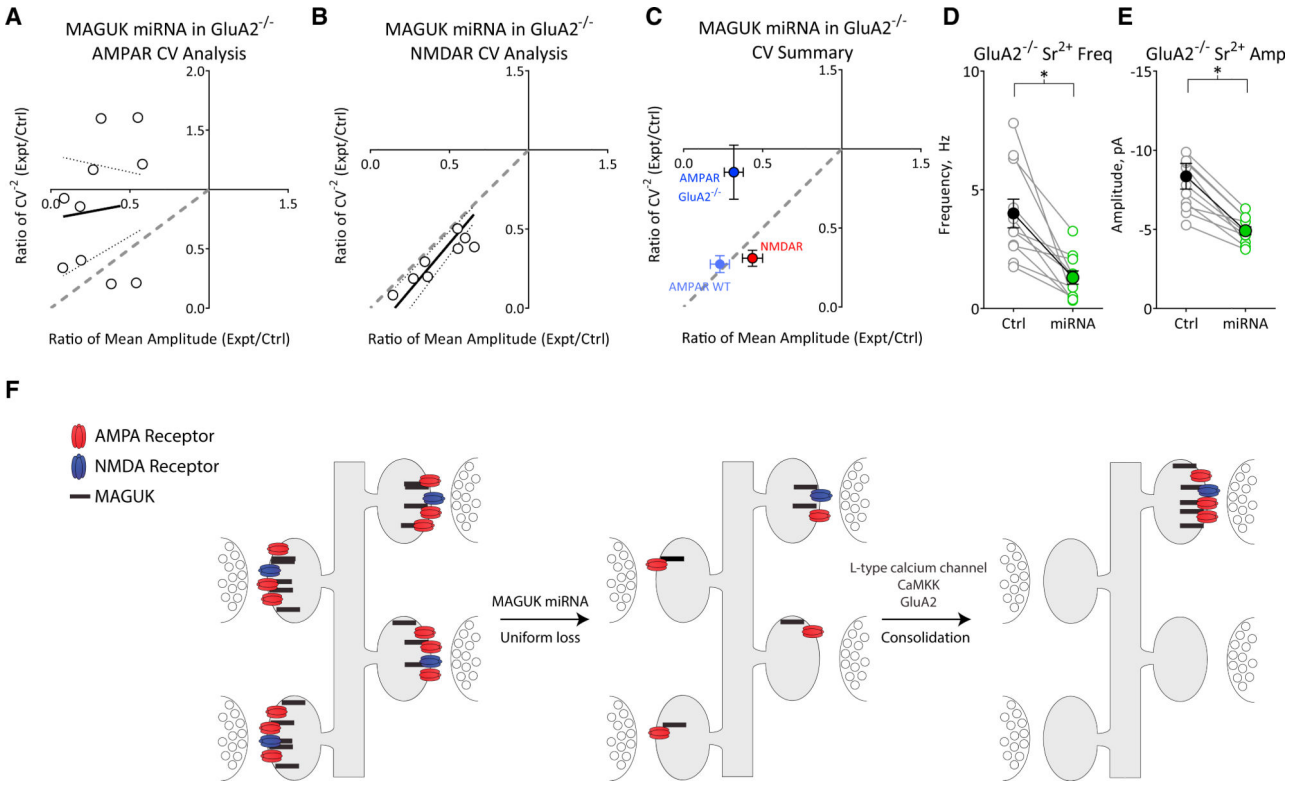

Figure 7. GluA2 AMPAR Subunit Is Required for Synaptic Consolidation

(A and B) Coefficient of variation analysis of simultaneously recorded pairs of control/miRNA neurons in GluA2 $^{-/-}$ slices. The decrease in AMPAR EPSC is due to reduction in quantal size and quantal content ($p < 0.01$ compared to horizontal line). The decrease in NMDAR EPSC is due to reduction in quantal content.

(C) Summary of coefficient of variation analysis. Data from MAGUK miRNA (Figure 4G) are re-plotted to aid comparison.

(D and E) Sr^{2+}-evoked aEPSC amplitude and frequency are reduced in neurons from GluA2 $^{-/-}$ slices shot with MAGUK miRNA compared to neighboring GluA2 $^{-/-}$ neurons ($p < 0.05$).

(F) Model of synaptic consolidation. MAGUK loss initially causes reductions in number of AMPARs present at individual synapses. Over time, compensatory processes normalize the number of AMPARs present at the few remaining synapses, at the cost of complete loss of other synapses. The glutamate receptors lost from synapses are re-distributed on the plasma membrane at extrasynaptic sites and have been omitted for clarity. The total number of surface-localized receptors remains unchanged. See also Figure S4.